

Supporting Information

Liu et al. 10.1073/pnas.1711734114

SI Materials and Methods

AO-OCT System Description. The AO-OCT system has been described previously (43, 44). For this study, the system used a single light source, a superluminescent diode with central wavelength of 790 nm and bandwidth of 42 nm, for AO-OCT imaging and wavefront sensing. Nominal axial resolution of the system in retinal tissue ($n = 1.38$) was 4.7 μm with depth sampling at 0.94 μm per pixel. The AO system consisted of a custom Shack–Hartman wavefront sensor and a deformable mirror (DM97; ALPAO) that dynamically measured and corrected ocular aberrations across a 6.7-mm pupil of the subject's eye. This resulted in a diffraction-limited lateral resolution of 2.4 μm . Image detection was based on a custom quad-spectrometer that was used in its two-camera mode that acquired A-scans at 500 KHz. The data stream from the AO-OCT system was processed and displayed real time to provide direct feedback. The system delivered <430 μW of power to the eye, an amount within safe limits established by the American National Standards Institute (49).

Determining Spatial Coordinates of GCL Somas. XYZ coordinates of GCL soma centers were identified and marked manually using software developed in MATLAB (The MathWorks Inc.). The software allowed visualization of cell somas in 3D by displaying simultaneously three orthogonal slices through the volume (one *en face* and two cross-sectional) that intersected at a common cursor point displayed as hair lines in each slice. The cursor was manually positioned at the center of a soma and, once confirmed in all three slices, its XYZ position was recorded and superimposed with an identifier marker. Subsequent somas were

identified and recorded in the same manner until all were marked in the volume.

Because of potential subjectivity in the manual selection of GCL soma centers, we tested for agreement between two trained technicians who independently mapped soma centers in six volumes, including several where the soma stack thickness reached a maximum of 4–5 near 3°. Average absolute difference between measurements was 1.8% in terms of *en face* cell density (mm^{-2}).

Quantifying Soma Reflectance. All somas were selected whose center coordinates fell within a narrow depth range (14 μm) that nominally bisected the GCL. This assured negligible influence of the AO-OCT's depth of focus on the reflectance measurement. The reflectance of each selected GCL soma was computed as an amplitude per pixel by averaging the reflectance in a $3 \times 3 \times 3$ pixel ($3 \times 3 \times 2.8 \mu\text{m}^3$) window centered on the XYZ coordinates of the soma.

Quantifying Soma CNR. Soma CNR was defined as the difference between the soma maximum and minimum amplitude divided by the SD of the soma noise. The SD was computed from the central 7×7 pixels ($7 \times 7 \mu\text{m}^2$) of the soma in the *en face* view, a sampling window small enough to avoid the soma edges. Because soma structure (not noise) also contributes to the SD, its contribution was estimated with a linear model of variance and subtracted. To see the effect of averaging on CNR, we varied the number of volumes averaged for a soma and computed the CNR for each average, and repeated the operation on different somas in the same retinal patch.

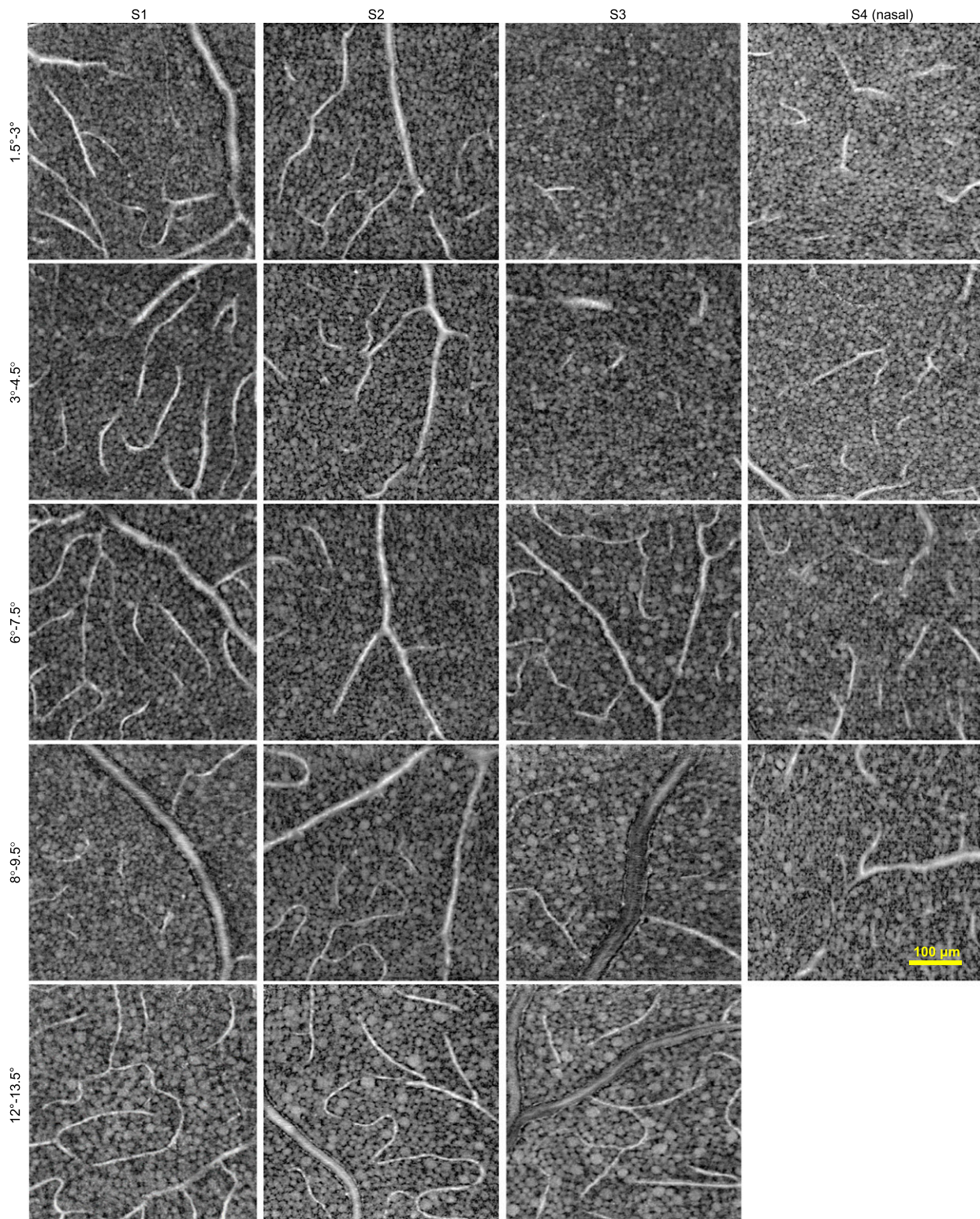


Fig. S1. AO-OCT *en face* cross-sections of the GCL as a function of retinal eccentricity in the four subjects. Mosaics of GCL somas, disrupted only by retinal vasculature, are observed in all subjects and retinal locations. Images are in temporal retina except S4. S4 temporal are in Fig. 3.

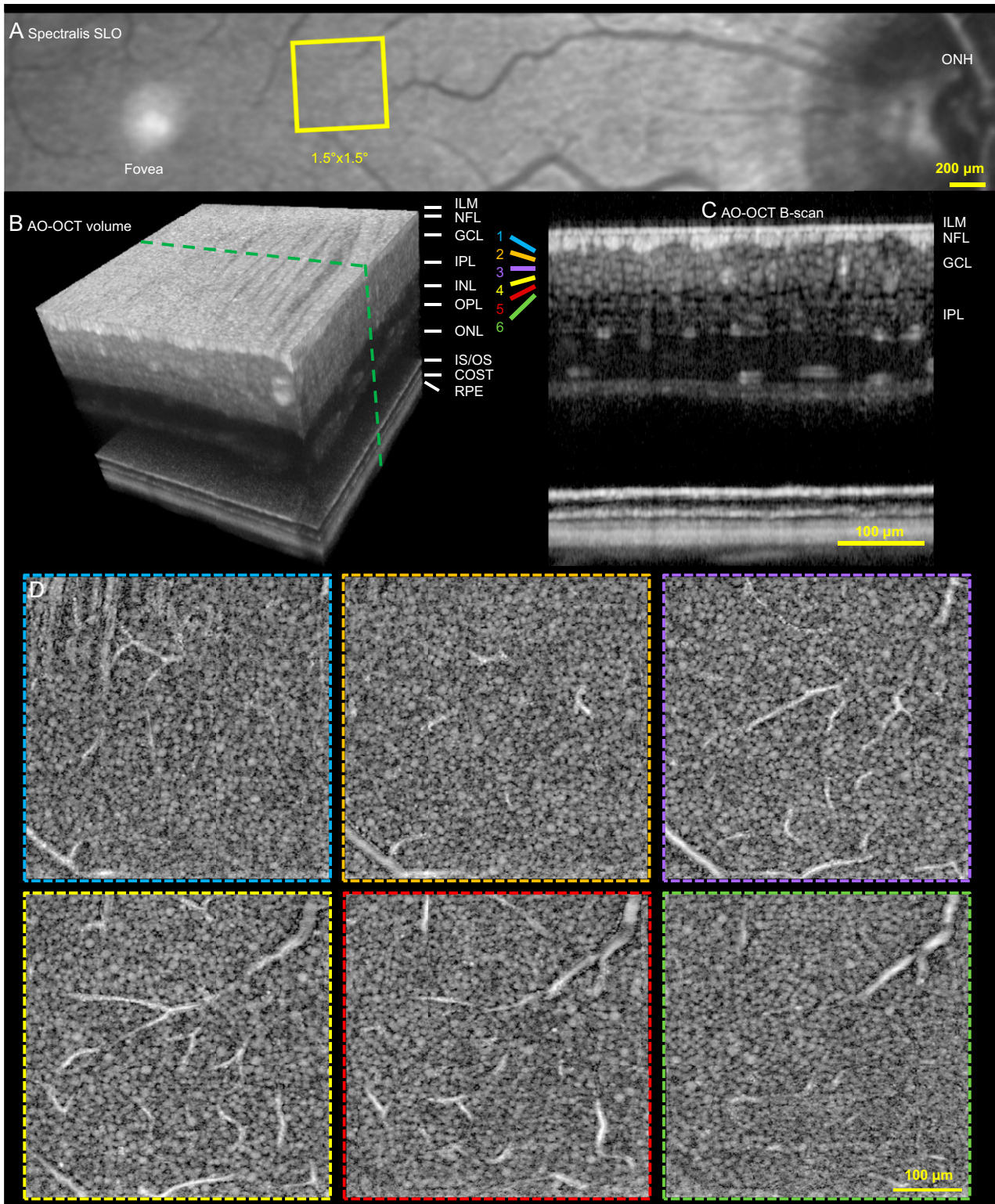


Fig. S2. AO-OCT volume reveals 3D stack of GCL somas under brightly reflecting NF bundles. (A) Yellow square at 3–4.5° nasal to the fovea in subject S4 denotes location imaged with AO-OCT. (B) Three-dimensional perspective of registered and averaged AO-OCT volume with green dashed line denoting cross-section of inner retina shown in C. (C) reveals soma stacks in GCL. (D) *En face* cross sections spaced 10 μm at increasing depth in GCL as color coded in C show a contiguous mosaic of somas. COST, cone outer segment tip; IS/OS, inner segment/outer segment junction; ONL, outer nuclear layer; OPL, outer plexiform layer (Movie S2).

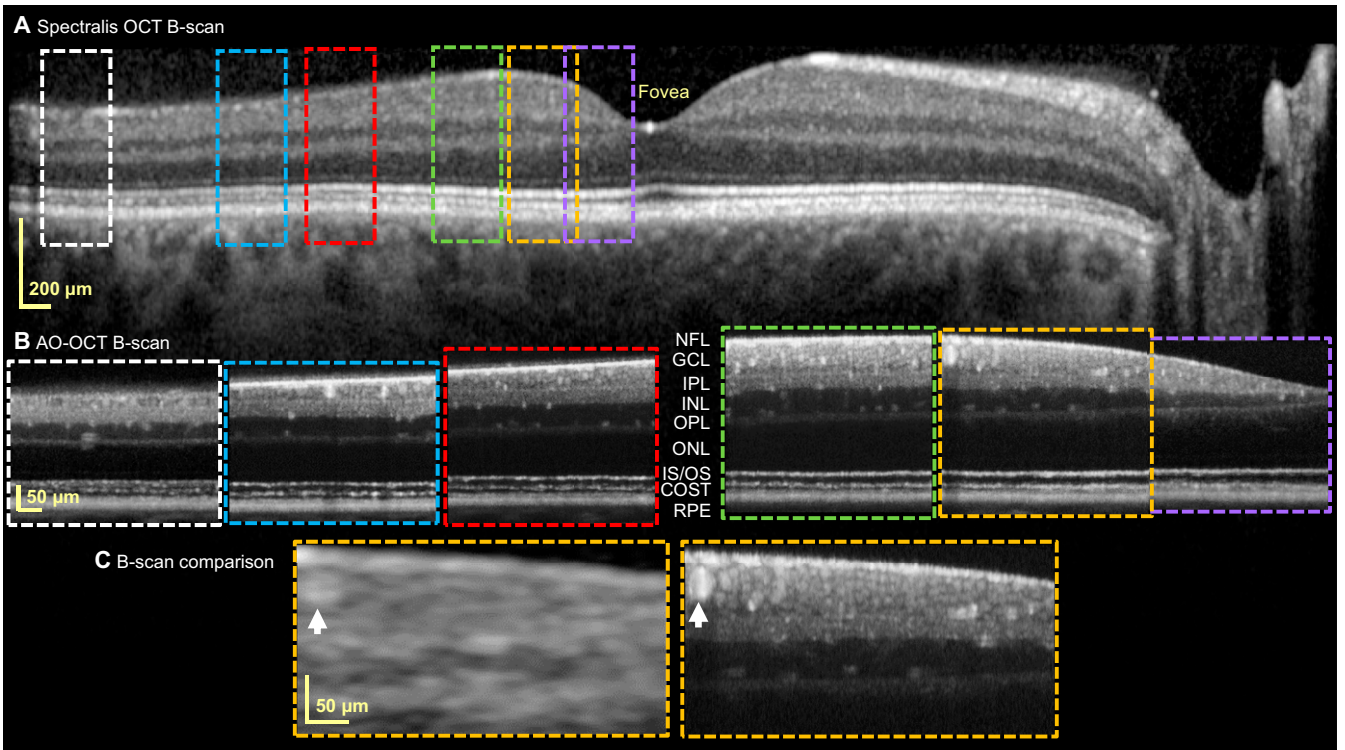


Fig. 53. Soma stack height in GCL varies with retinal eccentricity as revealed with AO-OCT, but not clinical OCT. (A) Clinical OCT B-scan with marks of the six retinal locations in subject S4 where AO-OCT volumes were acquired along the temporal, horizontal meridian of the macula. (B) Corresponding AO-OCT B-scans show variation of the soma stack thickness. (C) Side-by-side comparison of the clinical OCT and AO-OCT B-scans at 1.5–3° from A and B, respectively, demonstrate the resolution advantage of AO-OCT. White arrows point to the same blood vessel cross-section.

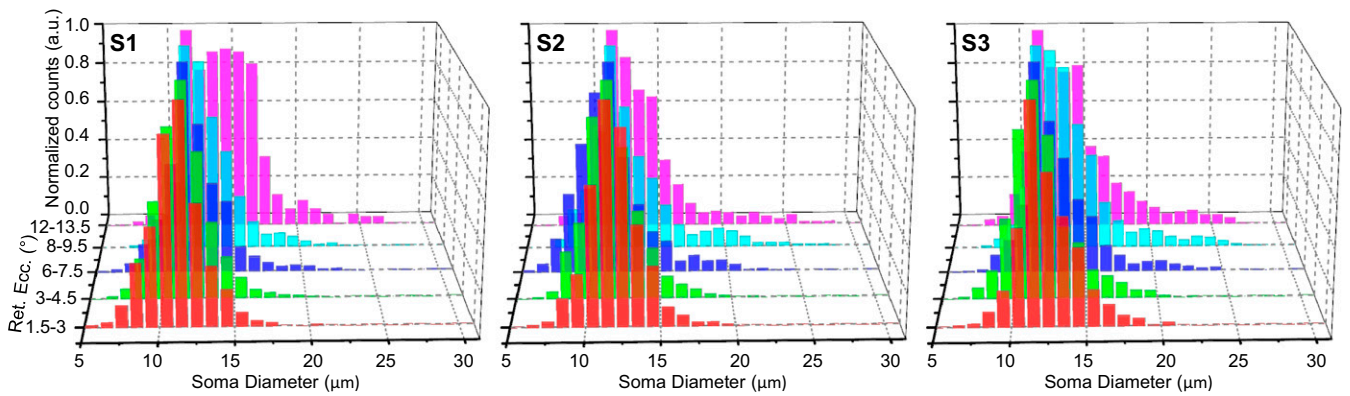


Fig. 54. GCL soma size distributions for three subjects (S1, S2, and S3) and color coded by retinal eccentricity. See Fig. 4 for S4 distribution.

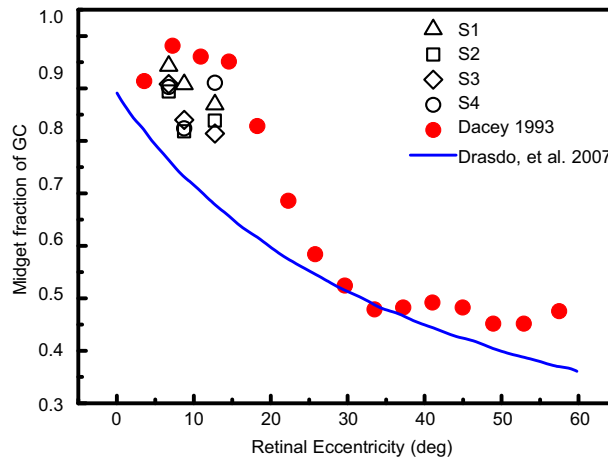


Fig. 55. Estimated fraction of GCs that are midget. AO-OCT estimates, from Gaussian fits of the bimodal size distributions, are plotted for the three largest retinal eccentricities imaged (6–7.5°, 8–9.5°, and 12–13.5°). Two histologic estimates (7, 20) are shown for comparison.

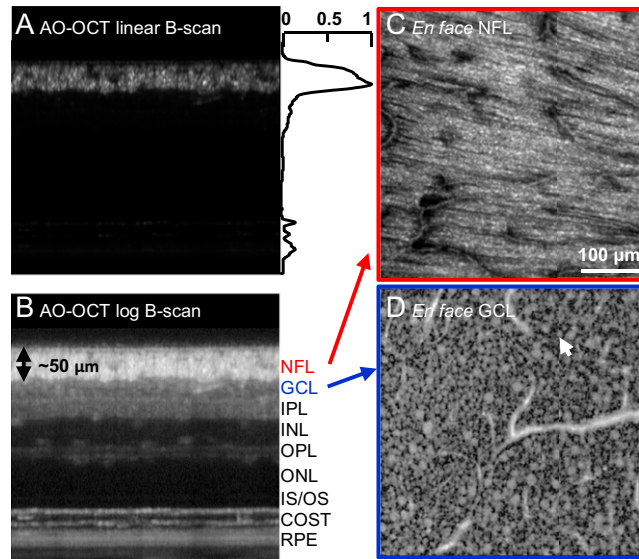


Fig. 56. GCL somas are visible beneath thick NFL. AO-OCT volume was acquired at 8–9.5° nasal to the fovea, a location near the nasal edge of the macula and adjacent to the optic disk. The AO-OCT linear amplitude B-scan (A), log B-scan (B), and en face image (C) confirm the extensive coverage of the NFL. (D) GCL en face image extracted beneath the NFL reveals a contiguous mosaic of GCL somas. White arrow points to an individual soma (Movie S3).

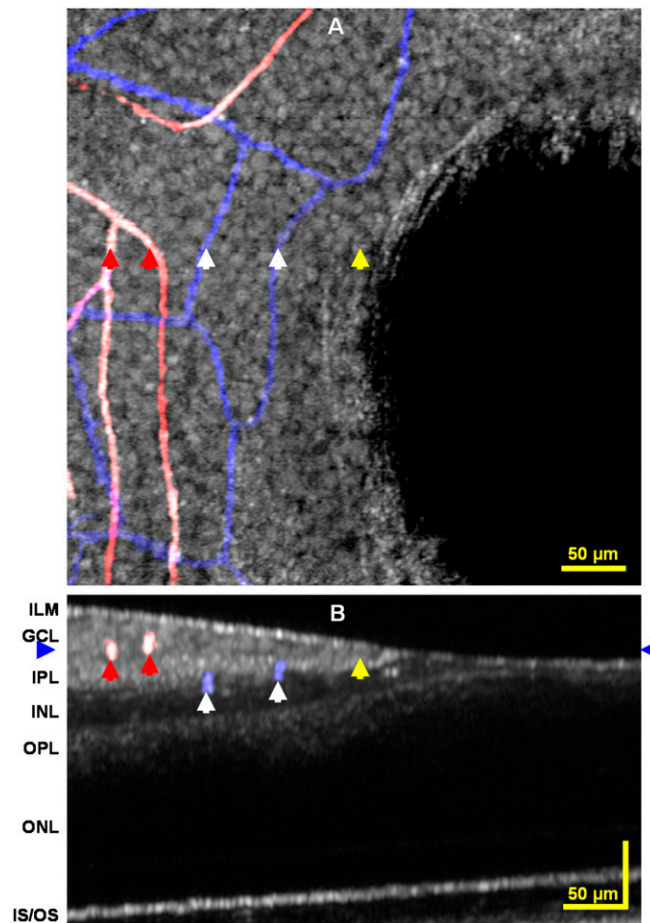
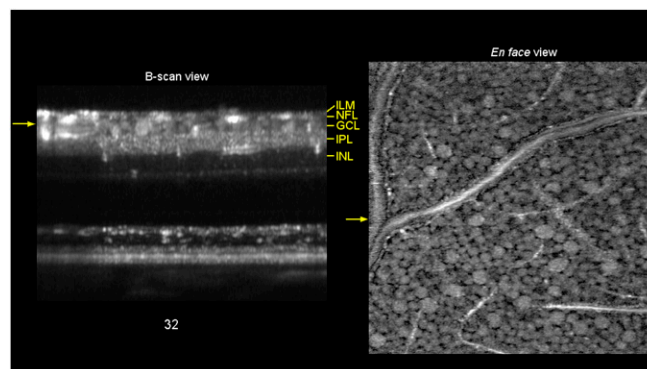
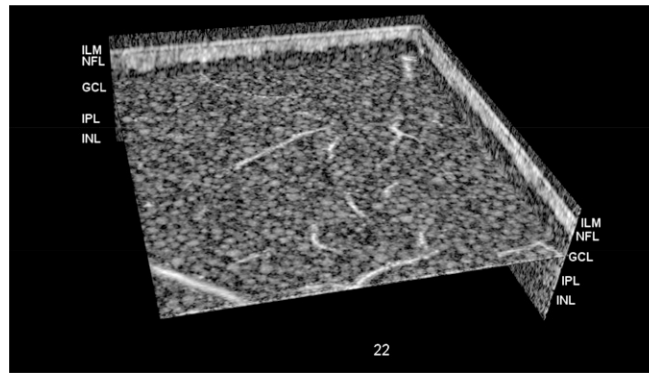


Fig. S7. Arrangement of GCL somas and retinal vasculature at the foveal rim. Soma mosaic extends into the foveal avascular zone in this AO-OCT volume acquired at $0.35\text{--}1.85^\circ$ temporal to the fovea in subject S1. (A) Superposition of three *en face* projections extracted from the volume: one at the posterior side of GCL that captures the single row of somas at the foveal rim (grayscale image), one at the GCL vasculature (red), and one at the IPL vasculature (blue). The bright vertical striations at the GCL foveal rim are likely part of the ILM, which is better appreciated in Movie S4. (B) The corresponding B-scan that aligns to the five colored arrows in the upper *en face* view shows the depth locations of the GCL somas and the retinal vasculature. The blue arrowheads located outside the B-scan indicate the retinal depth at which the *en face* GCL image in A was extracted. Yellow arrows in both images point to the GCL soma that is closest to the foveal center in the selected B-scan. Red and white arrows point to the blood vessels located in GCL (red) and IPL (blue), respectively.



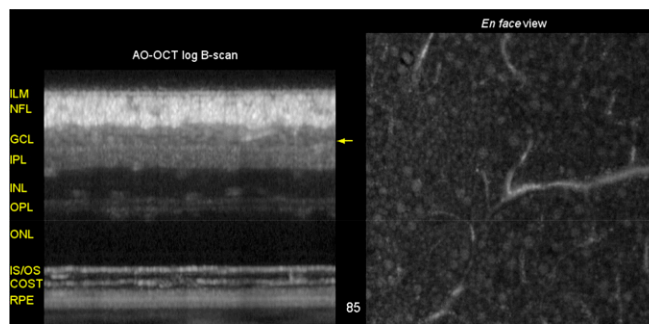
Movie S1. The rich cellular tapestry of the inner retinal layers as revealed with AO-OCT. *En face* flythrough of volume image acquired $12\text{--}13.5^\circ$ temporal to the fovea in subject S3. Frame numbers 10, 23, 32, and 56 correspond to the images in Fig. 2 D–G, respectively. Frames are $450 \times 450 \mu\text{m}^2$.

[Movie S1](#)



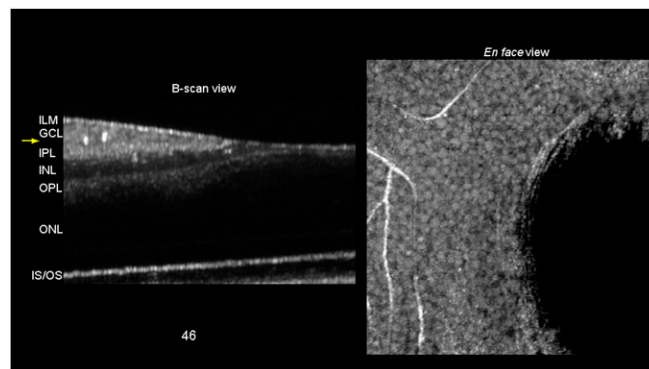
Movie S2. Stacked somas occupy the full GCL thickness. *En face* flythrough of volume image acquired 3–4.5° nasal to the fovea in subject S4. Frame numbers 17, 19, 22, 26, 29, and 30 correspond to the six images in Fig. S2D. Frames are $450 \times 450 \mu\text{m}^2$.

[Movie S2](#)



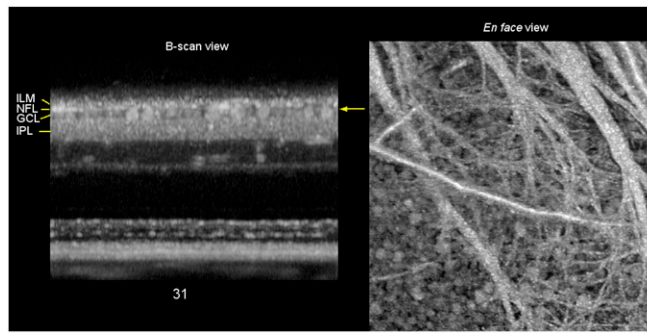
Movie S3. GCL somas underneath a thick NFL. *En face* flythrough of volume image acquired 8–9.5° nasal to the fovea and near the optic disk in subject S4. Frame numbers 33 and 85 correspond to images in Fig. S6 C and D. Frames are $450 \times 450 \mu\text{m}^2$.

[Movie S3](#)



Movie S4. Arrangement of GCL somas and retinal vasculature at the foveal rim. *En face* flythrough of volume image acquired 0.35–1.85° temporal to the fovea in subject S1. Frame number 46 corresponds to the GCL *en face* image in Fig. S7A. Frames are $450 \times 450 \mu\text{m}^2$.

[Movie S4](#)



Movie S5. Nerve fiber bundles dissipate into an intricate labyrinth of GC axons. *En face* flythrough of volume image acquired 12–13.5° temporal to the fovea in subject S4. Frame number 31 corresponds to the 12–13.5° image in Fig. 3. Frames are $450 \times 450 \mu\text{m}^2$.

[Movie S5](#)